A&A manuscript no.
(will be inserted by hand later)

Your thesaurus codes are:
011 (13.07.1; 13.25.1)

ASTRONOMY
AND
ASTROPHYSICS
1.2.2008

arXiv:astro-ph/9909465v1 28 Sep 1999

Inner accretion disk disappearance during a radio flare in GRS 1915+105

M. Feroci[1], G. Matt[2], G. Pooley[3], E. Costa[1], M. Tavani[4,5], and T. Belloni[6,7]

[1] Istituto di Astrofisica Spaziale, CNR, Via Fosso del Cavaliere, I-00133 Roma, Italy
[2] Dipartimento di Fisica, Universita' 'Roma Tre', Via della Vasca Navale 84, I-00146 Roma, Italy
[3] Mullard Radio Astronomy Observatory, Cavendish Laboratory, Madingley Road, Cambridge CB3 0HE, UK
[4] Istituto Fisica Cosmica e Tecnologie Relative, CNR, Via Bassini 15, I-20133 Milano, Italy
[5] Columbia Astrophysics Laboratory, New York, NY, USA
[6] Astronomical Institute "A. Pannekoek" and Center for High-Energy Astrophysics, Kruislaan 403, 109855 Amsterdam, The Netherlands
[7] Osservatorio Astronomico di Brera, Via Bianchi 46, I-23807 Merate, Italy

Received May 15, 1999; accepted September 28, 1999

Abstract.
Simultaneous X–ray (BeppoSAX, 0.1–300 keV) and radio (Ryle Telescope, 15 GHz) observations of the superluminal galactic source GRS 1915+105 in high flux state were carried out starting October 1996. The source was in a phase of large X–ray intensity and spectral variability. Among the simultaneous observations, an isolated radio flare lasting ∼2000 s was detected accompanied by X–ray outbursting activity. Here we present the simultaneous radio/X–ray light curves of the flare event and the spectral and timing analysis of the relevant BeppoSAX data. The broad band (0.1-200 keV) energy spectrum of the source can be described in terms of the 'standard' spectral model for black hole candidates. We obtain evidence for a temporary disappearance and subsequent restoring of the inner portion of the accretion disk during the flare from the spectral analysis of the X–ray data. We find a variable power law photon index positively correlated to the variability of the exponential cut-off energy. In addition, frequency and intensity variations of a ∼4-5 Hz quasi-periodic oscillation (QPO) are detected during the same time interval. The centroid frequency of the QPO is found to be correlated to the spectral power law photon index, and to the X–ray flux from the disk and the high energy flux from the power law. These observational results are discussed in the framework of the disk-instability model proposed for this source.

Key words: X-rays: observation – stars: individual: GRS 1915+105

Send offprint requests to: feroci@ias.rm.cnr.it

1. Introduction

GRS 1915+105 was discovered in X–rays in 1992 by the WATCH experiment onboard GRANAT (Castro-Tirado et al. 1992). It was then observed in the radio band, where plasma ejection activity with apparent superluminal motion was observed (Mirabel & Rodriguez 1994). This jet source, sometime referred to as a *microquasar* (due to a phenomenology analogous to a quasar but scaled down in mass by several orders of magnitude), is located close to the galactic plane, at a distance of ∼12 kpc as inferred from kinematic and HI measurements (Mirabel & Rodriguez 1994, Fender et al. 1999).

In X–rays GRS 1915+105 shows a wide range of variability on any sampled time scale. Quasi-periodic oscillations have been observed with the PCA experiment onboard the *Rossi X-ray Timing Explorer* (Greiner et al. 1997) at frequencies varying from a few mHz to 67 Hz (Morgan et al. 1997). The latter frequency, unlike all the others, does not change with time, and has therefore been suggested to be related with the innermost stable orbit of the accretion disk around the black hole (Morgan et al. 1997).

The X–ray spectrum of the source has been successfully described in terms of emission from an optically thick accretion disk (Belloni et al. 1997a). The disk emission is modelled as a multi-temperature blackbody of innermost temperature ∼1-2 keV. A population of energetic electrons can Compton up-scatter soft photons from the disk, thus originating the power law component observed in the spectrum. A low energy absorption is detected in X–ray observations, corresponding to a neutral hydrogen column of ∼5x10^{22} atoms

cm^{-2} (Greiner et al. 1997); the Galactic neutral hydrogen column to the source direction is $\sim$2x10^{22} atoms cm^{-2} (Dickey & Lockman 1990). The extreme variability of the source (both in flux and energy spectrum) has been interpreted (Belloni et al. 1997a) in terms of a cycle consisting of the abrupt emptying of the inner portion of the accretion disk followed by a slower refilling (Belloni et al. 1997b).

Radio maps have shown that during its active phases the source often exhibits events of plasma ejections, observed as extended radio flux emission. In some cases the outflowing plasma propagates through the interstellar medium for tenths of a parsec, with an intrinsic velocity of 0.92-0.98 c and apparent superluminal motion (Mirabel & Rodriguez 1999, Fender et al. 1999). Using simultaneous observations at different wavelengths, several authors (Pooley & Fender 1997, Fender et al. 1997, Fender & Pooley 1998, Eikenberry et al. 1998a, Mirabel et al. 1998, Eikenberry et al. 1998b, Fender et al. 1999) were able to correlate the X–ray variability with the emission at radio and infrared frequencies. In particular, they showed that the observed multi-frequency behaviour is consistent with a scenario in which instabilities in the inner portion of the accretion disk, detected as oscillations of the X–ray flux, cause a plasma jet ejection that adiabatically expands away from the source. The radio and infrared radiation detected from the jets is consistent with a synchrotron emission mechanism.

2. Observations

A Target of Opportunity observational campaign (Feroci et al. 1998, Matt et al. 1998) with the Narrow Field Instruments (NFI: LECS, MECS and PDS, Boella et al. 1997) onboard BeppoSAX started after its Wide Field Cameras (2–26 keV, Jager et al. 1997) detected intense X–ray activity from this source. After two observations of about 10 ks, the source was observed continuously with the NFI for more than one day (Fig. 1), and then monitored again for two more weeks with a series of short observations. Along with the BeppoSAX observations, radio monitoring of GRS 1915+105 was performed at the Ryle Telescope at 15 GHz (Pooley & Fender 1997), resulting in a sparse set of short X–ray/radio simultaneous observations.

In this paper we discuss one of such observations, during which a radio flare was detected simultaneously with an isolated X–ray outbursting activity of the source. The X-ray spectral and timing characteristics are of particular interest and, as we will show, can be interpreted in terms of the sudden disappearance of the inner portion of the accretion disk. The analysis of the remaining observations will be presented in a forthcoming paper.

2.1. The flare event

On 1996 November 1.628 UT, GRS 1915+105 exhibited the X–ray outburst shown in Fig. 2 (top panel) and 3. The source was in a high-flux ($\sim 2.3\times10^{-8}$ erg cm^{-2} s^{-1} in 2–10 keV), relatively quiet state when the outburst occurred; during the outburst large amplitude oscillations were observed (Fig. 3). After that, the source went into a dip and finally recovered a state similar to that before the outburst. On a longer timescale, the event occurred after a period of relatively quiet X-ray behaviour (at high flux level) following an impressive flaring state lasting almost one day (Fig. 1, Feroci et al. 1998). This temporal behaviour may be seen in context of the scenario described in Belloni et al. (1997a). At the time of the X–ray outburst the inner portion of the disk undergoes an instability that, in few hundred seconds, leads to its disruption, causing a decrease in the emitted X–ray flux. The instability results in ejection of plasma out of the inner disk. Once the instability is damped, the inner accretion disk is replenished and the X–ray emission restored.

The 15 GHz radio emission during the same time period is shown in the bottom panel of Fig. 2. At the time of the X–ray outburst (in a period unfortunately not fully covered by the X–ray observation due to the Earth occultation), the radio emission shows a smooth, relatively fast rise followed by a slower decay. The radio flux increase is almost linear with time, reaching a peak flux of $\sim$ 60 mJy in correspondence with the X–ray dip. The decay from this peak follows a quasi-exponential law down to a flux of $\sim$ 20 mJy, when the radio observation stops. The time profiles in the two bands are rather different, being more complex in X-rays than in the radio.

In the correlated X–ray and radio events studied so far (Pooley & Fender 1997, Mirabel et al. 1998, Eikenberry et al. 1998b) the source exhibited a series of X–ray flares and dips. The corresponding radio and infrared flares have been interpreted (e.g., Mirabel & Rodriguez 1999 and references therein) in terms of emission from plasmoids ejected at the time of the preceding X–ray dips, with the relative X-ray/infrared/radio delay due to the optical thinning during adiabatic expansion of the plasma bubbles. However, we note that in that observations the relative phase between the X–ray and radio/IR light curves is not always the same. In some cases (see Fig. 2 of Mirabel et al. 1998) the radio peak is reached during the X–ray outburst, but in several other cases (see Fig. 5 of Pooley & Fender 1997, Fig. 1 of Mirabel et al. 1998 and Fig. 2 of Eikenberry et al. 1998, if one extrapolates that the radio peaks after the IR) the radio emission peaks during the X-ray dip, just like we observe. Of course, these differences can be attributed to casual superpositions of uncorrelated events, due to the intense activity of the source. In this scenario, it is possible that the correlation

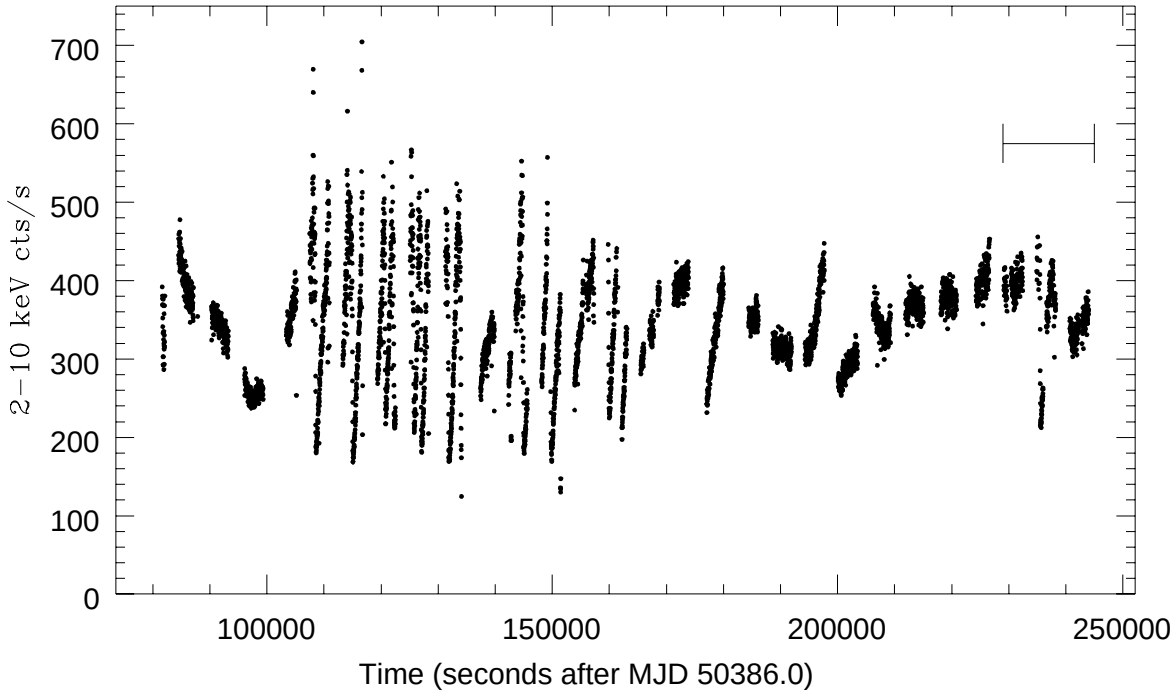

Fig. 1. BeppoSAX MECS (2–10 keV, bin size 16 s) light curve of the long observation of GRS 1915+105, showing the source behaviour before the occurrence of the outburst shown in figure 2. The time interval shown in Figure 2 is indicated here with an horizontal line. Data gaps are due to Earth occultation and to passages of BeppoSAX close to the South Atlantic Anomaly.

between X–rays and radio emission that we observed (i.e. the radio peak at the time of the X–ray dip) is also fortuitous, and the radio event is actually associated with the dip of an unseen X–ray flare occurred during the data gap due to Earth occultation (i.e. between intervals A and B in Fig. 2). However, we note that in this case one would naturally expect also a radio event following the observed X–ray event. This is not seen, unless this putative radio flare is blended with the decay of the main radio event. The latter hypothesis would in turn likely require that the unseen X–ray outburst is much larger than the observed one (if a relation exists between the X–ray flare intensity and the radio emission intensity).

Alternatively, if we use only the information directly derived from our observations and assume that the radio flare is actually associated to the observed X–ray flare, we may suppose that we are dealing with a somewhat different event with respect to those interpreted in the literature, or with the same phenomenon on a smaller scale (and therefore a shorter time scale). This may not be too much surprising also looking at the context in which the X–ray flare occurred (Fig. 1): it appears to be rather isolated in a period of relative stillness of the X–ray emission, while the events usually discussed in the literature occurred in periods of high X–ray variability, within long and continuous sequences of flares and dips individually similar to the one we show here (i.e., a period like the first half of our long observation, Fig. 1). In fact, it is known that some radio flares from this and similar sources are not related to substained plasma emission forming a steady jet, being instead exhausted at an early stage ('aborted events', that is, small versions of the big ejections with spectacular jets; R. Hjellming, private communication). Suppose we are dealing with one of these 'aborted jets', during the high frequency oscillations (interval B and earlier) relatively small plasmoids are ejected out of the disk, rapidly becoming optically thin and being therefore observable at radio frequencies. In this scenario, the observed radio peak would simply be the convolution of individual plasmoid's emission ejected in a sequence which ceased at the time of the X–ray dip (when the inner accretion disk disappears, see below), causing the subsequent decrease in the radio flux.

We assume this scenario as our working hypothesis. In the next section we will test the inner disk disappearance hypothesis using a spectral modeling of the 0.1–

200 keV X–ray emission observed with BeppoSAX during the event. Then, in the following section we search for timing signatures in the X–ray data.

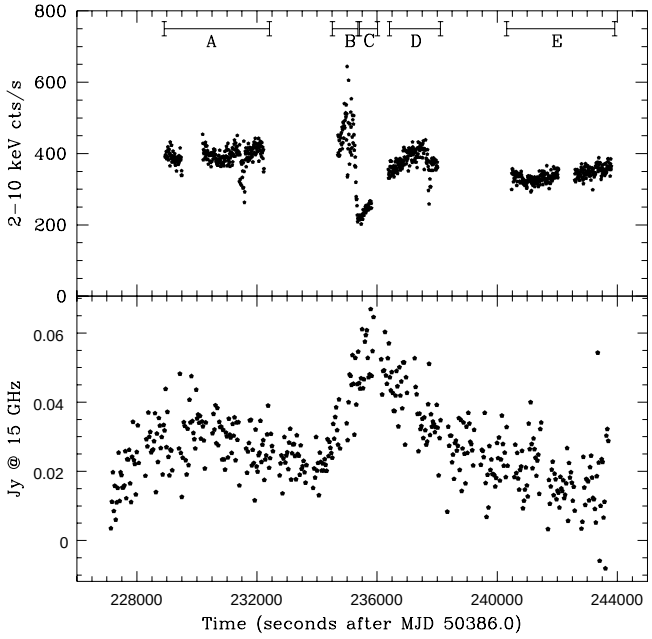

Fig. 2. BeppoSAX MECS (2–10 keV, bin size 10 s) and Ryle Telescope (15 GHz, 32 s bin size) light curve of the flare from GRS 1915+105. The data gaps in the X–ray light curve are due to the satellite passage near the South Atlantic Anomaly and to Earth occultations.

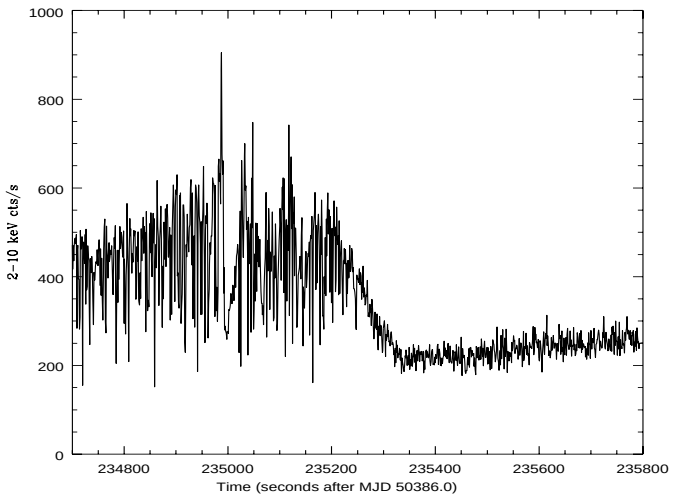

Fig. 3. Zoom-in (bin size 1 s) of the MECS light curve of the outburst reported in Fig. 2, showing the complex timing behaviour of the source during the time intervals B and C. For this figure it looks very likely that the high frequency oscillations started earlier than the beginning of interval B, during the Earth occultation

3. Broad band spectral analysis

In order to infer the source behaviour from the BeppoSAX spectral data we divided the observation in five time intervals (A, B, C, D, E) as shown in Fig. 2. The aim of this time selection was to divide the event on the basis of the source state. We note, however, that the chosen time intervals could include significant spectral variation of the source, as suggested by Fig. 3 for interval B, and the results that we derive could represent 'average states' of the source.

The available spectral data from the BeppoSAX observation are from the LECS instrument (0.1–4 keV) for portions of the A, D and E intervals; from the MECS (1.8–10 keV) and from the PDS (15–200 keV) for all the five intervals. In the spectral analysis with these three instruments we used a normalization factor for the intercalibration with the MECS (Fiore et al. 1999): 0.84 (fixed) for the PDS, free parameter for the LECS (usually between 0.9 and 1.0). The LECS data have been mainly used to determine the column density of the absorbing matter, which has been found to be constant in the three available time intervals at the value of $\sim 5.6 \times 10^{22}$ cm^{-2}. Since LECS data are available only for portions of only 3 of the 5 selected intervals, in order to avoid systematic differences in the data analysis between spectra with and without the LECS we fitted only MECS and PDS data, with the neutral hydrogen column density fixed to the value derived from the LECS.

For the spectral fitting (performed with the XSPEC v. 10 package, Arnaud 1996) we used a model including the following components: a multi-temperature disk blackbody, a power law with a high energy exponential cut-off, an iron emission line and a Compton reflection continuum from cold matter (assuming an inclination angle of 70°). This model was typically used for black hole candidates (Mitsuda et al. 1984), and it is the same used in Belloni et al. 1997a to fit RXTE/PCA data, except for the high energy cut-off and the Compton reflection that we added due to the wider (0.1–300 keV) BeppoSAX spectral coverage. The use of the Compton reflection component (with the high energy cut-off included in the relevant *XSPEC* model) is generally preferred to a simple cut-off power law when fitting the BeppoSAX wide band energy spectra (not only those presented in this paper) of this source. Actually, it is also used to fit RXTE data when also the high energy instrument, HEXTE, is used (Greiner et al. 1998). However, this component is not always well constrained. As an example, in case of interval E if we change the Compton reflection to a cut-off power law, we pass from χ^2=149.1 (89 d.o.f.) to χ^2=161.7 (90 d.o.f.), and an F-test at-

tributes a probability of 99.3% of improvement to the use of the Compton reflection model.

In Fig. 4 we show the best-fit models to the data of the five selected time intervals, showing both the individual components and the total spectrum. For the sake of clarity we did not show real data in this figure, whose purpose is to show the evolution of the individual spectral components. As an example of the statistical quality of our data we show the actual data for interval E - for which we also have data from the LECS - in Fig. 5, together with the best fit model and residuals (we note that this is one of the cases with the worse χ^2).

In Tables 1 and 2 we report the spectral fit parameters (all errors are given at a 90% confidence level, unless otherwise specified).[1] A word a caution is necessary here for what concerns the physical meaning of the inner disk radius and temperature. First of all, general relativity effects (e.g. Zhang et al. 1997) are not included in the adopted model (*diskbb* in *XSPEC*). For instance, as discussed by Sobczak et al. (1999a, 1999b), the relativistic corrections imply a radius of the innermost stable orbit smaller than what derived from this model. Also, the *diskbb* model may be not appropriate to describe the source energy spectrum in some conditions (see also Merloni et al. (1999) for a critical discussion of this effect), resulting in an unrealistic value for the inner disk radius. Therefore, the values of inner radius given in Table 2 have to be regarded with extreme caution. (We note, however, that these effects do not substantially affect our observational evidence of the lack of the thermal component during interval C.)

In Table 2 and Fig. 4 it is immediately evident that the soft thermal component (the disk) significantly contribute to the spectrum in intervals A, B, D and E, while in the dip (interval C) it is not required by the data. During the outburst (interval B) it shows the largest intensity and temperature, while it appears basically constant in A, D and E. The power law component also shows significant variations. In particular, the power law photon index varies only slightly along the event, but for the interval C where it shows a increase of ∼0.3-0.4. Correspondingly, the high energy cut-off shows a significant increase, passing from ∼50-60 keV to ∼100 keV. Unfortunately, the parameter uncertainties for the Fe line and the reflection component are too large to search for possible variability.

[1] Even if the value for the reduced χ^2 is rather high in some intervals, namely A and E, we were not able to get better fits, either changing parameters or changing the model. We therefore think that these values are due to intrinsic rapid variation of the continuum on timescales shorter than those used here (∼500-3000 s), and/or to residual systematic uncertainties in the deconvolution matrices of the instruments, because of the high intensity of this source. We stress, however, that we just used the statistical counting errors in the fit, without adding any systematic error.

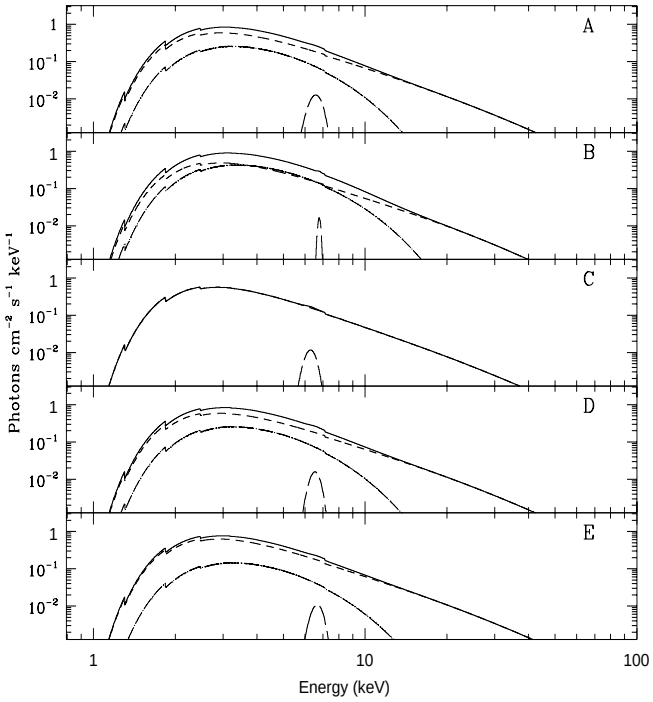

Fig. 4. Best fit models for the broad band BeppoSAX spectra in the five sections shown in figure 1. The model include an absorbed ($N_h \sim 5.6 \times 10^{22}$) power law with a high energy cut-off and a Compton reflection component from a disk (dashed curve), a multi-temperature disk blackbody (dot-dash), and an Iron line (long dash). The continuous line shows the sum of the various components.

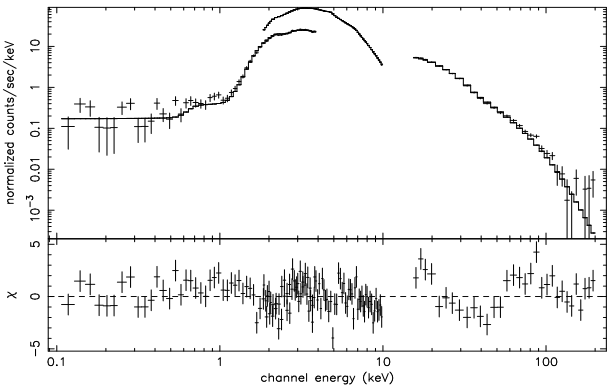

Fig. 5. Data and best fit model for the broad band BeppoSAX spectrum of interval E. Count-rates from all the three instruments (LECS, MECS and PDS) are shown here together with their residuals with respect to the model (in units of individual contributions to the χ^2)

Table 1. Best-fit parameters for the continuum. The model includes an interstellar absorption (fixed at 5.6×10^{22} cm^{-2}, a power law with high energy cut-off, a Compton reflection component, an emission iron line and (except for interval C) a blackbody emission from a multi-temperature accretion disk. Errors are given at a 90% confidence level for one parameter.

Time Interval	Power law index	Cut-off Energy (keV)	Inner disk radius$^{(*)}$ (km)	Inner disk Temp. (keV)	Compton Reflection$^{(**)}$	Reduced χ^2 (d.o.f.)
A	$2.36^{+0.05}_{-0.04}$	$49.6^{+5.3}_{-3.9}$	$25.7^{+1.6}_{-1.7}$	$1.53^{+0.06}_{-0.05}$	< 0.36	1.99 (89)
B	$2.33^{+0.12}_{-0.08}$	$42.8^{+10.5}_{-6.4}$	$27.0^{+1.7}_{-1.3}$	$1.69^{+0.05}_{-0.05}$	< 0.81	1.34 (89)
C	$2.68^{+0.03}_{-0.03}$	$94.3^{+29.6}_{-19.1}$	-	-	$0.47^{+0.30}_{-0.26}$	1.02 (92)
D	$2.44^{+0.07}_{-0.06}$	$58.8^{+9.5}_{-6.6}$	$26.4^{+2.5}_{-2.1}$	$1.51^{+0.07}_{-0.07}$	$0.41^{+0.35}_{-0.26}$	1.51 (89)
E	$2.53^{+0.04}_{-0.06}$	$70.2^{+9.1}_{-8.8}$	$19.5^{+3.9}_{-1.7}$	$1.52^{+0.08}_{-0.15}$	$0.47^{+0.24}_{-0.27}$	1.68 (89)

$^{(*)}$ Derived from the XSPEC model *diskbb*, assuming a distance of 12 kpc and a inclination angle to the disk of 70°
$^{(**)}$ Dimensionless parameter *rel_refl* of the XSPEC *pexrav* model, corresponding to the solid angle subtended by the reflecting matter to the illuminating source in units of 2π

Table 2. Best-fit parameters for the iron line. The model is the same as in Table 1.

Time Interval	E_{line} keV	σ keV	Line flux 10^{-2} ph/cm^2/s	Equivalent width eV
A	$6.57^{+0.14}_{-0.14}$	$0.35^{+0.19}_{-0.19}$	$1.25^{+0.67}_{-0.50}$	45
B	$6.72^{+0.28}_{-0.29}$	< 0.48	$0.57^{+0.64}_{-0.45}$	19
C	$6.29^{+0.24}_{-0.25}$	0.3 (fix)	$0.97^{+0.41}_{-0.41}$	55
D	$6.53^{+0.11}_{-0.20}$	< 0.56	$1.24^{+0.88}_{-0.63}$	45
E	$6.65^{+0.13}_{-0.25}$	$0.35^{+0.41}_{-0.20}$	$1.00^{+1.28}_{-0.41}$	44

Table 3. Best-fit values used for the correlation presented in Fig. 8 and 9: QPO centroid frequency, power law flux (2-10 keV), flux (2-10 keV) from the multi-temperature disk blackbody and power law flux (15-50 keV)

Time Interval	QPO Centroid Frequency^a (Hz)	PL flux^b (2-10 keV)	DBB flux^b (2-10 keV)	PL flux^b (15-50 keV)
A	5.23±0.11	2.71	1.05	0.70
B	-	2.25	1.82	0.59
C	4.12±0.18	2.36	-	0.47
D	5.16±0.13	2.62	1.04	0.69
E	4.58±0.08	2.74	0.59	0.65

^{a} The centroid value was obtained from a gaussian+polynomial fit to the QPO peak and the local underlying continuum. The confidence level of the associated error is 3σ.
^{b} Unabsorbed flux in units of 10^{-8} erg cm^{-2} s^{-1}, corresponding to a luminosity of $\sim 1.6\times10^{38}$ erg s^{-1}

4. Timing analysis

We used the MECS (1.8–10 keV) data to study the temporal behaviour of the source in the five intervals. The MECS light curves where produced with a 3 ms bin size. Using the Xronos package (v. 4.02) we divided the light curves in time segments ∼12 s long and calculated the power density spectrum for each of them. The spectra reported in Fig. 6 are then obtained averaging a minimum of ∼40 power density spectra (up to 280 for the longest interval).

A peaked feature is detected at a frequency between 4 and 5 Hz, varying both in frequency and intensity over the 5 intervals. We interpret such a feature as a quasi-periodic oscillation (QPO) of the 'intermediate type' (Morgan et al. 1997, Markwardt et al. 1999, Muno et al. 1999). The QPO is detected at 5.23 Hz in interval A, then is not detected during the outburst (interval B), it appears again at 4.12 Hz during the dip (interval C), and moves to 5.16 Hz and 4.58 Hz during intervals D and E, respectively. It is interesting to note how the feature gets sharper in interval E, while it seems broader in interval C. In this interval the QPO peak could actually be the convolution of a variable peak QPO, as suggested by observations of similar source states by RXTE (e.g., Markwardt et al. 1999, Muno et al. 1999), where the QPO frequency is observed to drift in time on very short timescales. Also, it is worth noting the possible existence of a small peak in interval A at a frequency ∼2.6 Hz, possibly a sub-harmonic of the QPO as observed in other black hole candidates (see van der Klis 1995 for a review).

It is worth noticing that the shape of the low frequency continuum is significantly different in interval C

(the dip, during which the disk component is not detected in the energy spectrum), where it is much flatter than in the other intervals, particularly with respect to B (the outburst) where it appears the highest.

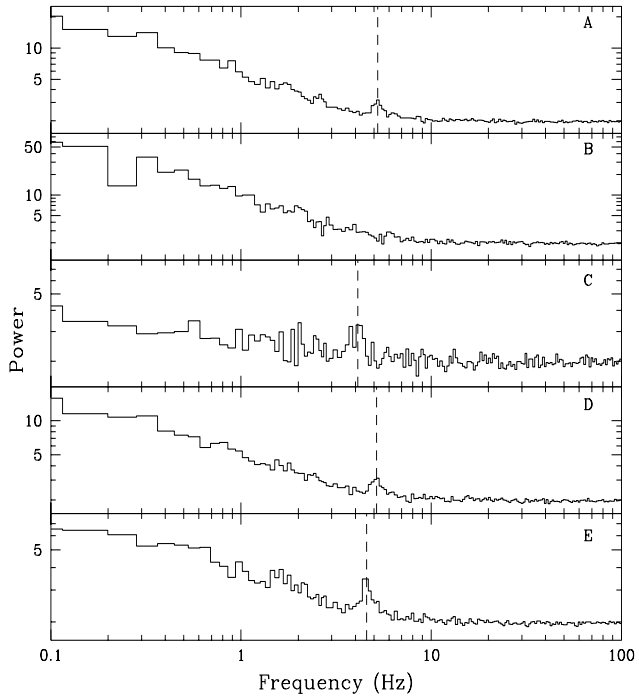

Fig. 6. Power Spectral Density obtained by the MECS data for the five intervals given in Fig.2. Frequency bins are spaced according to a geometric series. The vertical dashed lines indicate the centroid of the QPO frequency at 5.23 Hz (A), 4.12 Hz (C), 5.16 Hz (D) and 4.58 Hz (E).

5. Discussion

The spectral analysis of the BeppoSAX X–ray data confirmed that the radio/X flare event that we observed is consistent with the scenario, proposed by Belloni et al. (1997a), in which X-ray outbursts occur when the inner part of the accretion disk is disrupted, and plasma is expelled out of the disk, thus generating the radio peak observed at 15 GHz. The global behaviour of the spectral parameters is also consistent with what found by Trudolyubov et al. (1998) on similar source states.

We studied possible correlations between spectral and timing parameters. First, we find that the photon index of the power law component appears to be positively correlated with the cut–off energy (Fig. 7). A word of caution is necessary here, as the two parameters are strongly correlated in the fit procedure, and this is exactly the kind of correlation that could arise if the power law index were wrongly estimated for some unknown reason. On the other hand, as we will show below the power law photon index appears well correlated to temporal parameters too, which have been derived from a completely independent analysis. Even if this cannot be considered as a proof, it is nevertheless a suggestion in favour of the correctness of the measurement of the power law indices, and therefore of the reality of the correlation. We have also searched the literature for a confirmation of this effect. Heindl et al. (1997) and Muno et al. (1999) use data from the HEXTE experiment onboard RossiXTE. In table 2 of the former paper we find only two useful fits, and they are consistent with our correlation. In table 3 of Muno et al. (1999) we find six spectral fits in which our correlation is not found. However, we note that the value of the cut-off energy in the latter analysis is always larger (∼100 keV, and not far from the upper energy bound of the data set) than what we find, while Heindl et al. (1997) obtain values similar to ours (60 and 88 keV).

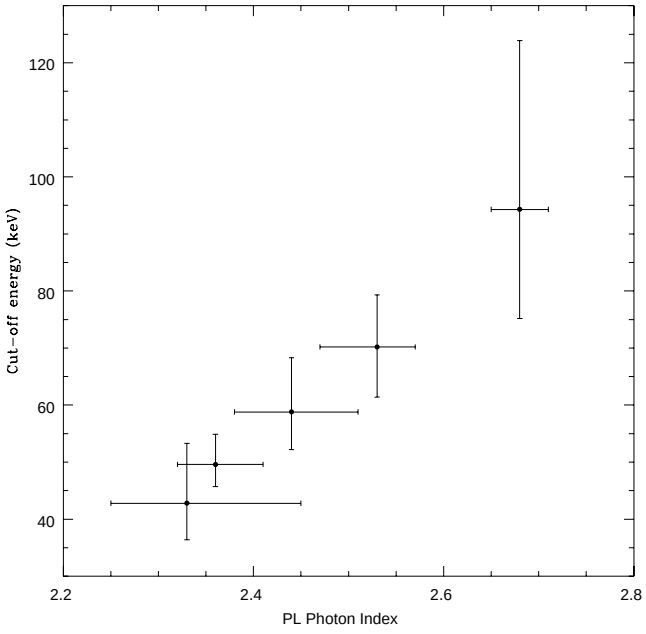

Fig. 7. Correlation between the power law photon index and the high energy cut-off

The timing analysis of our X–ray data shows the presence of a variable QPO around 5 Hz. This frequency is classified as 'intermediate' in the phenomenology of this source, and the centroid frequency is usually observed to vary between 1.5 and 15 Hz. Trudolyubov et al. (1998) and Muno et al. (1999), analysing data from RossiXTE with the source in a variety of spectral and intensity states, found positive correlations of the inter-

mediate QPO centroid frequency with the low energy flux from the power law component and from the thermal disk emission. Also, Markwardt et al. (1999) found a correlation between the frequency of the intermediate QPO and the parameters of the disk component.

In our data set a negative correlation exists between the QPO centroid frequency and the power law photon index (Fig. 8). Given the correlation between the power law index and the cut-off energy it is also possible that the real correlation is between the QPO frequency and the cut-off energy. In principle, it could be related to the already known QPO-flux correlation, but we only find a correlation between the QPO centroid frequency and the flux in the 2–10 keV from the disk blackbody and in the 15–50 keV from the power law component (Fig. 9). On the contrary, there is not clear correlation with the low energy (2–10 keV) flux from the power law component, even if our small data set does not allow to definitely rule it out. This may be explained if the basic correlation is with the photon index, and the power law is pivoting at low energies; actually, the variation in the 2–10 keV flux is significantly lower than in the 15–50 keV flux.

We note that our results on the correlations of the QPO centroid frequency with the disk blackbody flux and the high energy power law flux are in agreement with what found by Muno et al. (1999) using RXTE data, while the anti-correlation with the power law index is opposite to what can be inferred by using the different correlations presented by these authors. This might be a chance occurrence due to our small data set or an intrinsic difference due to the fact that the analysis of the RXTE data includes a large number of observations and source states, whereas our data refer to a single flare event and are integrated over longer time segments.

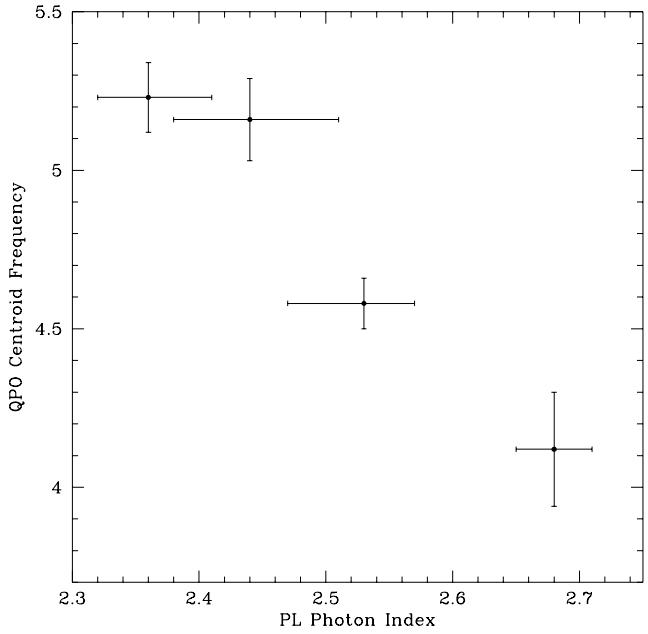

Fig. 8. Correlation between the power law photon index and the centroid frequency of the QPO

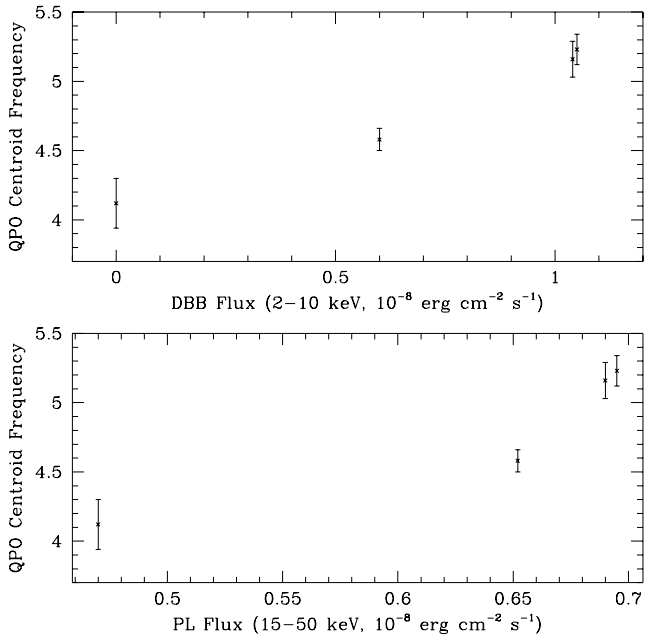

Fig. 9. *Top Panel:* Correlation between the 2-10 keV flux from the multi-temperature disk blackbody and the centroid frequency of the QPO
Bottom Panel: Correlation between the flux in the 15-50 keV range from the power law and the centroid frequency of the QPO

6. Conclusions

Our observations clearly indicate that the GRS 1915+105 system is subject to overall instabilities affecting both the disk and its surroundings. We studied an isolated radio flare (possibly caused by an expanding cloud of energized electrons emitting at large distance from the central object) associated with an isolated X–ray outbursting activity followed by a shallow dip. It is remarkable that the relative timing of the radio and X–ray flare in this episode appears possibly different from what seen in some observations presented in the literature (see Sect. 2.1). The X–ray outbursting episode (lasting in our data ~ 600 s) appears to be chaotic with rapid fluctuations that most likely coincide with the energization of an external corona and of the radio emitting electrons. The ultimate cause of this instability is unknown. Several suggestions have been proposed, including thermal/viscous disk instabilities (Taam et al. 1997) and/or turbulent magnetic field dissipation in the inner part of the accretion disk (Tavani & Liang 1996). The

different states that we observe for the power law component might be caused by a quasi-thermal and moderately thick Comptonizing corona, or by an optically thin and magnetically energized particle population radiating by synchrotron and/or inverse Compton. Our observations do not favor one or the other mechanism.

Based on the observational results obtained from both the spectral and timing analysis of the BeppoSAX data, we try to phenomenologically interpret the observed source behaviour in the framework of the model proposed by Belloni et al. (1997a). The relevant observational results are:
(a) a correlation exists between the QPO centroid frequency and the spectral parameters of both the disk and the power law component;
(b) the disk emission is maximum during the X–ray outburst (interval B);
(c) high amplitude, fast oscillations are detected in X–rays during the outburst;
(d) the QPO is absent during the outburst;
(e) the low-frequency noise is maximum during the flare and it is minimum during the dip;
(f) the disk emission disappears during the dip (interval C);
(g) the lowest QPO frequency is observed during the dip;
(h) the cut-off energy jumps to its highest value during the dip;
(i) the radio emission rise together with the X–ray outburst, and peaks during the dip;
(l) the thermal disk emission is restored after the dip (intervals D and E).

Our point (a) indicates that the three observed source characteristics (disk emission, power law emission, QPO) either originate from the same site, or in different sites causally related with each other. (For example, it has been proposed (Chakrabarti et al. 1995, Molteni et al. 1996, Kazanas et al. 1997, Titarchuk et al. 1998) that a 1–10 Hz QPO might originate from radial oscillations at a boundary between the optically thick accretion disk and an extended atmosphere of hot electrons, responsible for the power law emission through comptonization of soft disk photons.)

At the time of the outburst the disk undergoes violent instabilites (point c) causing plasma emission out of the disk. The thermal emission from the disk is therefore reinforced by the plasma emission (point b). When the plasma is ejected into the extended atmosphere it goes through the boundary region where the QPO might take place, disturbing the dynamical equilibrium that generates it, and causing its temporary disappearance (point d). After the plasma jet ejection the internal disk no longer exists/emits (point f). The ejected plasma has thus caused an increase of the average energy of the coronal electron population, detected both as an increase of the cut-off energy (point h), and as a smooth increase of the radio synchrotron emission (point i) that reaches its peak when the ejection of plasma out of the disk ends. The dynamical equilibrium at the boundary region, temporarily perturbed by the plasma ejection event, is now being restored. The quasi-periodic oscillation therefore starts again, but it is at a lower frequency (point g), possibly due to a a larger distance from the central object, as also suggested by Muno et al. (1999) who find a positive correlation between the innermost disk temperature and the QPO frequency. Then, at the time of intervals D and E, a new dynamical equilibrium is reached when the inner disk is filled again and is detectable at X–rays (point l). It is also interesting that the low-frequency noise appears significantly lower when the inner disk is absent and maximum when the emission from the disk is at its highest value (point e), demonstrating that this timing feature is associated with the inner disk.

Therefore, the results obtained from our analysis of an isolated flare are consistent with a 'complete cycle' of an accretion disk perturbation, causing the temporary disappearance of the inner portion of the disk, within a scenario in which the accretion disk and the Comptonizing electrons population are geometrically or physically related. The interaction between the two would be therefore responsible for the quasi-periodic oscillation of intermediate (∼5 Hz) frequency. The even more complex behaviour often observed in this source, could then be a combination (with possible modifications and complications and on different timescales) of cycles similar to the one observed here.

Acknowledgements. We wish to thank R. Hjellming for useful discussions about radio jets and the anonymous referee for comments that helped to improve the clarity of the paper. The BeppoSAX Science Operation Center and Science Data Center assisted the authors during the observations and data reduction. EC, MF and GM acknowledge financial support by ASI and MURST.

References

Arnaud, K.A., 1996, Astronomical Data Analysis Software and Systems V,
eds. J. Jacoby and J. Barnes, ASP Conf. Ser. 101, 17
Belloni, T., M. Mendez, A.R. King, M. van der Klis and J. van Paradijs, 1997a, ApJ, 479, L145.
Belloni, T., M. Mendez, A.R. King, M. van der Klis and J. van Paradijs, 1997b, ApJ, 488, L109.
Boella, G. et al. 1997, A&ASS, 122, 299
Castro-Tirado, A.J., S. Brandt and N. Lund, 1992, IAU Circular n. 5590
Chakrabarti, S., and Titarchuk, L., 1995, ApJ 455, 623
Dickey, J., and Lockman, F., 1990, ARA&A. 28, 215
Eikenberry, S.S., et al., 1998a, ApJ 494, L61
Eikenberry, S.S., et al., 1998b, ApJ 506, L31
Fender, R.P., Pooley, G.G., Brocksopp, C., Newell, S.J., 1997, MNRAS 290, L65

Fender, R.P. and Pooley, G.G., 1998, MNRAS 300, 573
Fender, R.P., et al., 1999, MNRAS 304, 865
Feroci, M., Costa, E., Matt, G., Belloni, T., and Tavani, M., 1998, Nucl. Phys. B (Proc. Suppl.) 69, 336
Fiore, F., Guainazzi, M., and Grandi, P., 1999, *Cookbook for BeppoSAX NFI Spectral Analysis*, version 1.2, 7 January 1999
Greiner, J., E.H. Morgan and R.A. Remillard, 1997, ApJL 473, L107
Greiner, J., E.H. Morgan, and R.A. Remillard, 1998, New Astronomy Reviews, 42, 597
Heindl, W.A., et al., 1997, AIP Conf. Proc. 410, 897
Jager, R., et al. 1997, A&ASS, 125, 557
Kazanas, D., Hua, X.-M., and Titarchuk, L., 1997, ApJ 480, 735
Markwardt, C.B., Swank, J.H. and Taam, R.E., 1999, ApJ 513, L37
Matt, G., Costa, E., Feroci, M., Belloni, T., and Tavani, M., 1998, New Astronomy Reviews, 42, 625
Merloni, A., Fabian, A.C., and Ross, R.R., 1999, submitted to MNRAS
Mirabel, I.F., and L.F. Rodriguez, 1994, Nature 371, 46
Mirabel, I.F., et al., 1994, AA 282, L17
Mirabel, I.F., et al., 1998, AA 330, L9
Mirabel, I.F., and L.F. Rodriguez, 1999, ARA&A *in press* (astro-ph/9902062)
Mitsuda, K., et al., 1984, PASJ, 36, 741.
Molteni, D., Sponholz, H., and Chakrabarti, S.K., 1996, ApJ 457, 805
Morgan, E.H., R.A. Remillard and J. Greiner, 1997, ApJ 482, 993
Muno, M.P., Morgan, E.H., and Remillard, R.A., preprint (astro-ph/9904087)
Pooley, G.G., and Fender, R.P., 1997, MNRAS 292, 925
Sobczak, G., et al., 1999a, ApJ 520, 776
Sobczak, G., et al., 1999b, preprint (astro-ph/9903395)
Taam, R.E., Chen, X., and Swank, J.H., 1997, ApJ 485, L83
Tavani, M., and Liang, E., 1996, AAS 120, 133
Titarchuk, L., Lapidus, I., and Muslimov, A., 1998, ApJ 499, 315
Trudolyubov, S., Churazov, E., and Gilfanov, M., 1998, preprint (astro-ph/9811449)
van der Klis, M., 1995, *Rapid aperiodic variability in X–ray binaries* in *X–Ray Binaries*, W.H.G. Lewin, J. van Paradijs and E.P.J. van den Heuvel eds., Cambridge Univ. Press
Zhang, S.N., Cui, W., and Chen, W., 1997, ApJ 482, L155

This article was processed by the author using Springer-Verlag LaTeX A&A style file *L-AA* version 3.